Research Paper

Lateral orbitofrontal dysfunction in the *Sapap3* knockout mouse model of obsessive–compulsive disorder

Huimeng Lei, PhD; Juan Lai, MS; Xiaohong Sun, BS; Qunyuan Xu, MD, PhD; Guoping Feng, MD, PhD

Published online Nov. 7, 2018; subject to revision

Background: Obsessive–compulsive disorder (OCD) is a common psychiatric disorder that affects about 2% of the population, but the underlying neuropathophysiology of OCD is not well understood. Although increasing lines of evidence implicate dysfunction of the orbitofrontal cortex (OFC) in OCD, a detailed understanding of the functional alterations in different neuronal types in the OFC is still elusive. **Methods:** We investigated detailed activity pattern changes in putative pyramidal neurons and interneurons, as well as local field potential oscillations, in the lateral OFC underlying OCD-relevant phenotypes. We applied in vivo multichannel recording in an awake OCD mouse model that carried a deletion of the *Sapap3* gene, and in wildtype littermates. **Results:** Compared with wildtype mice, the lateral OFC of *Sapap3* knockout mice exhibited network dysfunction, demonstrated by decreased power of local field potential oscillations. The activity of inhibitory and excitatory neurons in the lateral OFC showed distinct perturbations in *Sapap3* knockout mice: putative interneurons exhibited increased activity; putative pyramidal neurons exhibited enhanced bursting activity; and both putative pyramidal neurons and interneurons exhibited enhanced discharge variability and altered synchronization. **Limitations:** To exclude motor activity confounders, this study examined functional alterations in lateral OFC neurons only when the mice were stationary. **Conclusion:** We provide, to our knowledge, the first direct in vivo electrophysiological evidence of detailed functional alterations in different neuronal types in the lateral OFC of an OCD mouse model. These findings may help in understanding the underlying neuropathophysiology and circuitry mechanisms for phenotypes relevant to OCD, and may help generate and refine hypotheses about potential biomarkers for further investigation.

Introduction

Obsessive–compulsive disorder (OCD) is a debilitating neuropsychiatric condition with a lifetime prevalence of 2%.[1] It is characterized by persistent intrusive thoughts (obsessions) and repetitive actions (compulsions). Although dysfunction of the cortico–striato–thalamo–cortical circuitry has been implicated in the pathogenesis of OCD[2–5] and is supported by neuroimaging studies in patients,[6–9] the underlying neuropathological changes are still not well understood. The orbitofrontal cortex (OFC) may be central to our understanding of OCD, because it is the most frequently reported region of structural, functional and connectivity alterations in patients with OCD.[10–12] The OFC is thought to update outcome expectations when rules linking stimuli to outcomes are changed.[13–15] Therefore, the OFC is essential for behaviour flexibility and goal-directed behaviours, both of which are impaired in people with OCD.[16,17] For this reason, the OFC is well suited as a neural substrate for OCD pathogenesis.

Although a large number of functional neuroimaging studies have shown altered metabolic activity in the OFC of people with OCD, a detailed understanding of the functional alterations is still elusive. For example, a majority of studies have reported increased resting metabolic activity in the OFC of people with OCD,[18–22] which is exacerbated by symptom provocation[23,24] and alleviated after successful treatment.[25–30] However, these studies can only measure metabolic levels to indirectly reflect general neuronal activity levels. The noninvasive methods used in clinical studies also have limited spatial and temporal resolution. Direct electrophysiological evidence of detailed activity change of different neuronal types in the OFC of people with OCD or animal models is still lacking. Furthermore, there are discrepancies in the directionality of findings in clinical neuroimaging studies that may be due

Correspondence to: H. Lei, Department of Neurobiology, Capital Medical University, You An Men Wai, Xi Tou Tiao, No. 10 Beijing, Beijing 1000069, China; leihm@ccmu.edu.cn; G. Feng, McGovern Institute for Brain Research, Department of Brain and Cognitive Sciences, Massachusetts Institute of Technology, Cambridge, MA 02139; fengg@mit.edu.

Submitted Feb. 28, 2018; Revised May 18, 2018; Accepted Jun. 27, 2018

DOI: 10.1503/jpn180032

to the heterogeneity of the disorder, comorbidities, medication history or different subregions of the OFC analyzed.

In the present study, we investigated detailed functional change in different neuronal types in the lateral OFC (lOFC) that underlie OCD-relevant phenotypes by applying in vivo multichannel recording in an awake OCD mouse model that carried a deletion of the *Sapap3* gene. These *Sapap3* knockout (KO) mice demonstrate several OCD-like behaviours, including excessive and pathological self-grooming and increased anxiety-like behaviours, suggesting potential relevance to OCD. As well, the entire constellation of OCD-like behaviours in *Sapap3* KO mice is alleviated by chronic fluoxetine, a first-line treatment for OCD.[31] Human genetics studies also support a role for *Sapap* genes in OCD.[32–34] Therefore, a detailed understanding of functional alterations in the OFC of *Sapap3* KO mice could help identify potential circuit mechanisms for behaviours relevant to OCD. The OFC consists of lateral and medial subregions. The lateral and medial OFC may perform different functions, such as processing negative versus positive valence.[35,36] A previous study from our group found that selective stimulation of the lOFC suppressed overexpression of both spontaneous and conditioned repetitive grooming behaviours, suggesting involvement of the lOFC in these behaviours in *Sapap3* KO mice.[37] To investigate functional alterations in the OFC in *Sapap3* KO mice, we focused on the lOFC subregion in the current study. Using single-unit and local field potential (LFP) recording in the lOFC, we studied activity pattern changes in different neuronal populations and alterations in LFP oscillations in *Sapap3* KO mice. Our goal was to shed light on the neuropathophysiology underlying OCD-like behaviours and advance our circuit-level understanding of phenotypes relevant to OCD. Our findings may help to generate and refine hypotheses for further investigation. For example, LFP alterations and increased burst firing in lOFC may be useful biomarker candidates for further examination in people with OCD.

Methods

Animal use

All experiments were conducted according to protocols approved by the Institutional Animal Care and Use and Institutional Biosafety committees of the Capital Medical University (Beijing, China) and the Massachusetts Institute of Technology (Cambridge, Massachusetts). Our group had previously found that from age 2 to 3 months, *Sapap3* KO mice exhibited significantly increased self-grooming that resembled compulsive OCD behaviours.[31] Therefore, we performed all of our experiments on adult *Sapap3* KO mice aged 3 to 10 months, and on age-matched, wildtype (WT) littermates of either sex.

Surgery

Our method of electrophysiological recording in head-restrained, mobile mice was based on previous studies with modifications.[38,39] Briefly, for head-plate implantation, mice were anesthetized by intraperitoneal injection of Avertin solution (20 mg/mL, 0.5 mg/g body weight) and then mounted in a stereotactic holder and kept warm (37°C) with an electric heating pad (BrainKing Biotech). A small skull region (~1 mm in diameter) located posterior to the lOFC based on stereotactic coordinates (anterior–posterior = 2.3 mm, medial–lateral = 1.3 mm) was thinned but not broken with a high-speed drill. A custom-made head plate with a hole 2 mm in diameter was placed on the skull, with the hole centred over the thinned region above the lOFC. The head plate was affixed to the skull with Meta-bond (Parkell Inc.), and the thinned skull and hole in the head plate were then covered with Kwik-sil (World Precision Instruments) for protection. Mice were individually housed after surgery and allowed to recover for 3 to 5 days before habituation training. To minimize potential stress effects, mice were trained to habituate to a head-fixed spherical treadmill for 2 to 4 hours each day for 4 consecutive days before recording. Mice quickly learned to balance and walk on the apparatus and stayed quiet for most of the time during recording, indicating low stress.

Electrophysiological recording

During electrophysiological recording, the mouse's head was restrained by a head plate, and the mouse was able to manoeuvre on the top surface of an air-supported floating styrofoam ball. Immediately before recording, we opened a small craniotomy in the thinned skull area above the lOFC. We detected extracellular spiking signals and LFP using a 32-channel silicon probe (A4×8–5mm-50–200–413-A32–15; NeuroNexus) arranged in a 4 × 8 pattern (4 shanks with 8 recording sites in each shank), lowered to the lOFC (anterior–posterior = 2.5–2.8 mm; medial–lateral = 1.0–1.6 mm, dorsal–ventral = 1.3–2 mm) and tilted rostrally at an angle of 15° to the vertical plane. Based on the above coordinates, we discarded neural activities recorded outside the lOFC from analysis. We sampled unit activity at 30 kHz and high-pass filtered it at 250 Hz using a Blackrock Cerebus data acquisition system (Blackrock Microsystems LLC). We sampled LFP at 1 kHz and low-pass-filtered it at 250 Hz. To avoid possible noise contamination in low-frequency oscillations, we discarded LFP data below 1.5 Hz.

Spike sorting and single-unit classification

We sorted unit activity containing spikes of multiple neurons manually offline using Offline Sorter (Plexon Inc.) and a combination of template-matching and principal-components analyses. A total of 362 single units were well isolated. Units with a trough half width within 100–200 μs, a peak half width within 467–700 μs and a trough:peak ratio within 1.2–2.8 were classified as putative pyramidal neurons. Units with a trough half width within 67–167 μs, a peak half width within 100–300 μs and a trough:peak ratio within 1.1–1.8 were classified as putative interneurons.[37,40] Using these criteria, we identified 294 units as putative pyramidal neurons and 51 units as putative interneurons.

Detailed explanations of these cell-type classification criteria are provided in Appendix 1, available at jpn.ca/180032-a1.

Statistical analysis

All analyses used custom Matlab software (H. Lei). For LFP oscillation power, the mean baseline firing rate of putative pyramidal neurons and interneurons, the percentage of spikes in the bursting mode per neuron and the number of bursts per minute per neuron, we determined statistical significance between WT and *Sapap3* KO mice using the Wilcoxon rank sum test. For LFP oscillation power, n was the number of animals. For single-unit activity, n was the number of neurons. We measured the correlation between firing rate and the depth of the neurons using the Spearman rank correlation coefficient.

We measured firing variability using C_{V2}.[41] We defined C_{V2} for spike i as the standard deviation of 2 adjacent interspike intervals (ISIs) divided by their mean and multiplied by √2.

$$C_{V2} = \frac{2|\Delta t_{i+1} - \Delta t_i|}{\Delta t_{i+1} + \Delta t_i}$$

Each C_{V2} corresponds to an ISI value that is the mean of the 2 adjacent ISIs used to compute C_{V2}. We computed mean C_{V2} by averaging all C_{V2} values corresponding to ISIs between a certain range. The ISI boundaries were logarithmically spaced with a ratio of 1.3. Because of the refractory period, we set the minimum ISI boundary at 1.69 ms. To access the significant difference of C_{V2} for different ISI ranges between WT and KO mice, we applied a Wilcoxon rank sum test to compare the mean C_{V2} values that corresponded to each ISI range. We then calculated the family-wise error rate to correct for multiple comparisons.

We calculated the spike-triggered average (STA) of the LFP at an interval of −5 s to 5 s, with LFP resampled at 200 Hz, so the bin size of the STA was 5 ms. We deemed STA fluctuation to be statistically significant when more than 10 consecutive bins (equal to a 50 ms time window) within an interval of −1 s to 1 s lay outside the minimum/maximum bound of its values at intervals of −5 s to −1 s and 1 s to 5 s. To access the significant difference for STA between WT and *Sapap3* KO mice, we applied the Wilcoxon rank sum test to the data points within the same corresponding bins of STA. If 20 or more consecutive bins had $p < 0.05$, we considered the STA during that time window to be significantly different.

Histology

To confirm recording location, mice were deeply anesthetized at the end of each recording (Nembutal, 50–100 mg/kg) and intracardially perfused with 50 mL 1 × PBS, followed by 50 mL 4% paraformaldehyde in PBS. Mouse brains were then postfixed in 4% paraformaldehyde/PBS overnight at 4°C and cryoprotected with 30% sucrose. Coronal sections were cut at 50 mm using a freezing microtome and reacted with Hoechst.

Results

Recording neuronal activity from the lOFC of awake mice

To identify changes in individual neuronal activity, we recorded extracellular single units and LFP from the lOFC of head-fixed, awake adult *Sapap3* KO mice (n = 24, 20 males and 4 females) and their age-matched, WT littermates (n = 21, 19 males and 2 females; Fig. 1A and B). Two-way analysis of variance (ANOVA) analysis showed a significant effect of genotype but no effect of sex (Appendix 1), so we pooled the data for male and female mice. To minimize stress, the mice were allowed to behave on an air-supported, frictionless spherical treadmill.[38] Because the activity of the lOFC is modulated by movement (Fig. 1C and D), we analyzed only the stationary epochs of the recordings to exclude movement or motor-directed activity confounders.

Reduced LFP oscillation power in the lOFC of Sapap3 *KO mice*

Brain rhythms are critical to coordinating the activity of neuronal populations across multiple spatial and temporal scales, and are involved in a wide range of cognitive and perceptual processes. To assess the rhythmic alterations of *Sapap3* KO mice, we recorded LFP at 64 sites, evenly distributed in a rectangular plane in the lOFC that was 600 µm in the medial–lateral dimension and 700 µm in the dorsal–ventral dimension, from a depth of 1300 µm to 2000 µm. We calculated the LFP power for each mouse by averaging the recordings across the 64 sites. The lOFC LFP oscillations in *Sapap3* KO mice exhibited reduced power at all frequency bands compared with their WT littermates (Fig. 2A and B). Specifically, the δ (1.5–4 Hz), θ (4–11 Hz), β (11–30 Hz) and γ (30–100 Hz) bands all had reduced power in *Sapap3* KO mice compared with WT mice (δ power normalized to WT mean: KO mean ± standard error of the mean [SEM] = 0.57 ± 0.05, WT = 1 ± 0.09, $p < 0.001$; θ power normalized to WT mean: KO = 0.59 ± 0.07, WT = 1 ± 0.09, $p < 0.001$; β power normalized to WT mean: KO = 0.54 ± 0.06, WT = 1 ± 0.11, $p < 0.001$; γ power normalized to WT mean: KO = 0.56 ± 0.06, WT = 1 ± 0.20, $p = 0.03$; Wilcoxon rank sum test; Fig. 2C, D, E and F). This is, to our knowledge, the first report of LFP alterations in the OFC in an OCD animal model. Because brain-rhythm alterations have been associated with several neuropsychiatric disorders including OCD,[42] alterations in OFC LFP oscillations may serve as a candidate biomarker to be further examined in people with OCD.

Increased activity of lOFC putative interneurons in Sapap3 *KO mice*

Brain rhythms are generated by the coordinated activity of multiple neuronal populations. The disrupted LFP oscillations found in the lOFC of *Sapap3* KO mice may indicate altered activity of multiple neuronal types. To dissect the role of individual neurons, we recorded a total of 362 single units that were isolated unambiguously using high spike-sort

quality. Among them, we recorded 215 single units from *Sapap3* KO mice: 182 were classified as putative pyramidal neurons and 30 were classified as putative interneurons, based on action potential waveforms. We recorded 147 single units from WT littermates: 112 were classified as putative pyramidal neurons and 21 were classified as putative interneurons (Fig. 3A and B).

The firing rate of putative interneurons while the mouse was at rest increased in *Sapap3* KO mice (WT mean ± SEM = 18.07 ± 1.50 Hz, median = 17.62 Hz; KO mean ± SEM = 22.56 ± 1.31 Hz, median = 23.30 Hz; p = 0.02 Wilcoxon rank sum test; Fig. 3C). Interestingly, however, the firing rate of putative pyramidal neurons at rest was unchanged between WT and *Sapap3* KO mice (WT mean ± SEM = 2.75 ± 0.30 Hz, median = 1.62 Hz; KO mean ± SEM = 2.78 ± 0.23 Hz, median = 1.50 Hz; p = 0.63 Wilcoxon rank sum test; Fig. 3D), suggesting intricate network imbalances in this mouse model with OCD-like behaviours. For both putative pyramidal neurons and interneurons, there was no correlation between firing rate and depth in either WT or *Sapap3* KO mice (Spearman rank correlation coefficient: WT putative interneurons r = 0.02, p = 0.94; KO putative interneurons r = 0.29, p = 0.12; WT putative pyramidal neurons r = −0.15, p = 0.11; KO putative pyramidal neurons r = −0.04, p = 0.57; Fig. 3E and F).

Increased bursting activity of lOFC putative pyramidal neurons in Sapap3 *KO mice*

The overall firing pattern (not merely the firing rate) determines neuronal function. Although we did not see any changes in the firing rate of pyramidal cells, we sought to compare their spike patterns between WT and *Sapap3* KO mice. In *Sapap3* KO mice, lOFC putative pyramidal neurons showed a notable enhancement of bursting activity compared with WT littermates (Fig. 4). Putative pyramidal neurons in *Sapap3* KO mice fired more bursts of doublet or triplet spikes with very short intra-burst ISI (< 10 ms). The number of bursts per minute per neuron was significantly increased

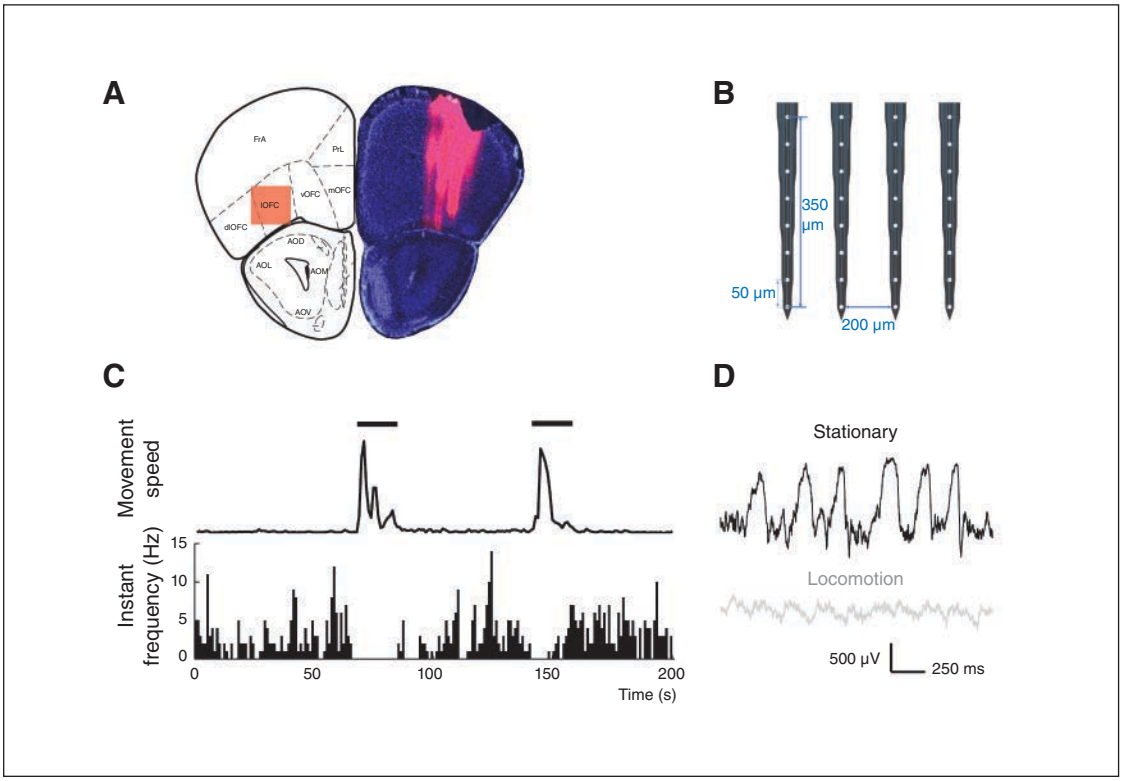

Fig. 1: Recording position and movement modulation of neuronal activity in lOFC. (**A**) Left: the red shadow summarizes the recording region, which was largely in the lOFC and sometimes also included the very medial portion of the dlOFC. Right: a histology example showing the tracks of the 4 electrode shanks reviewed by DiI (a fluorescent lipophilic cationic indocarbocyanine dye; red). (**B**) Electrode map. The recording electrodes had 4 shanks spaced by 200 µm. Each shank had 8 recording sites spaced by 50 µm. (**C**) An example of movement modulation of the spike activity of a putative pyramidal neuron in the lOFC of a WT mouse. This neuron decreased firing rate during locomotion. Horizontal bars indicate movement bouts. (**D**) An example of movement modulation of the LFP in the lOFC of a WT mouse. Black trace in the upper panel shows LFP when stationary. Grey trace in the lower panel shows LFP during locomotion. AOD = anterior olfactory area, dorsal part; AOL = anterior olfactory area, lateral part; AOM = anterior olfactory area, medial part; AOV = anterior olfactory area, ventral part; dlOFC = dorsolateral orbitofrontal cortex; FrA = frontal association cortex; LFP = local field potential; lOFC = lateral orbitofrontal cortex; mOFC = medial orbitofrontal cortex; PrL = prelimbic cortex; vOFC = ventral orbitofrontal cortex; WT = wildtype.

in *Sapap3* KO mice (WT mean ± SEM = 12.4 ± 1.9 times/min, median = 5.8 times/min; KO mean ± SEM = 18.2 ± 2.0 times/min, median = 10.7 times/min; $p = 0.001$, Wilcoxon rank sum test; Fig. 4C). The percentage of spikes per neuron in the bursting mode was also significantly increased in *Sapap3* KO mice (WT mean ± SEM = 22.9 ± 2.1%, median = 16.1%; KO mean ± SEM = 32.3 ± 1.8%, median = 29.0%; $p < 0.001$, Wilcoxon rank sum test; Fig. 4D). The intra-burst ISI was significantly shorter in *Sapap3* KO mice compared with WT mice (WT mean ± SEM = 6.60 ± 0.13 ms; KO mean ± SEM = 6.23 ± 0.09 ms; $p = 0.016$, Wilcoxon rank sum test). Bursts with short intra-burst ISI are more reliable and efficient for eliciting synaptic transmission than tonic firing.[43] Therefore, the increased bursting activity seen in *Sapap3* KO mice may enable lOFC pyramidal neurons to provide a stronger output and drive increased activity in the downstream structures of the orbito–fronto–striatal circuit in this OCD mouse model, reflecting specific pathologic neural processes in lOFC that underlie phenotypes relevant to OCD.

Increased firing variability for both neuronal types in Sapap3 *KO mice*

Both lOFC putative pyramidal neurons and interneurons in *Sapap3* KO mice exhibited enhanced discharge variability compared to WT littermates. To measure firing variability,

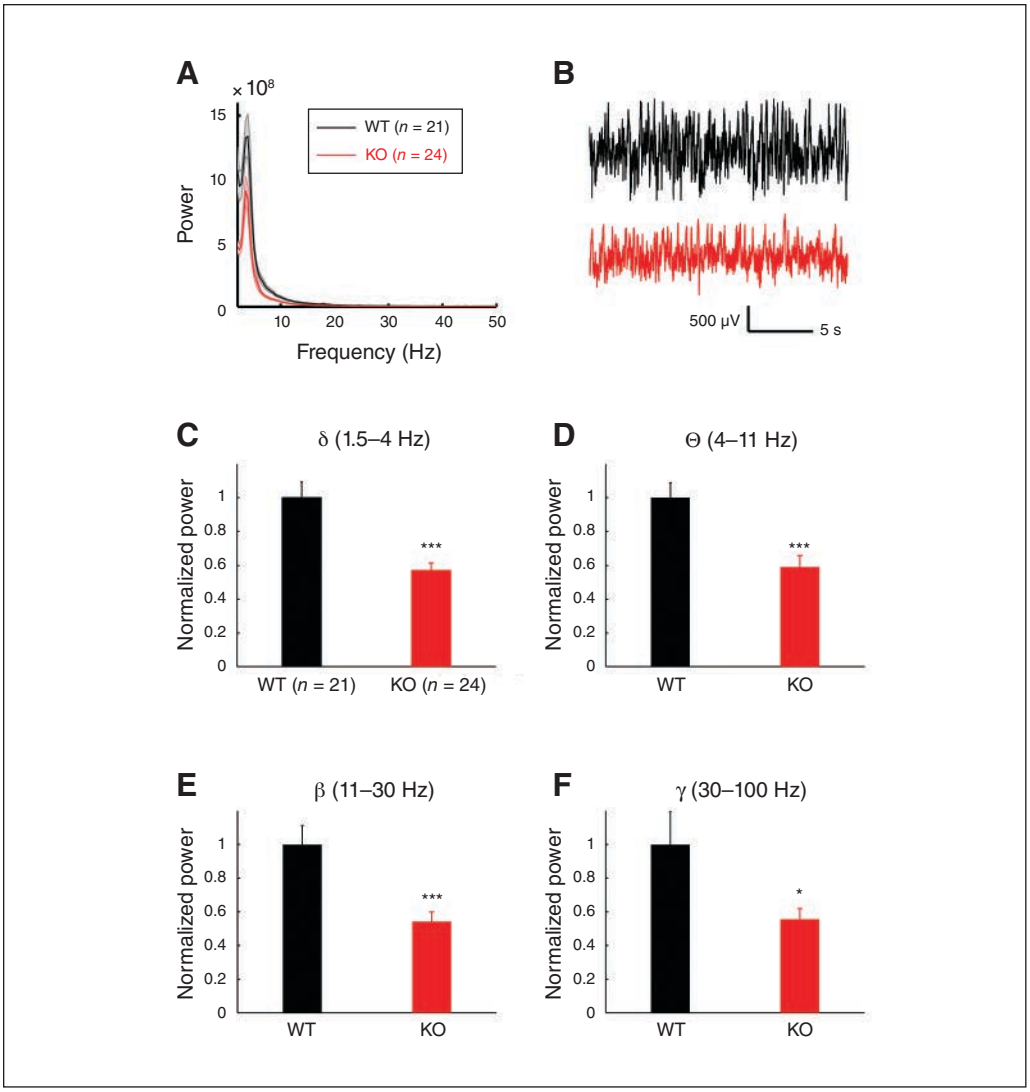

Fig. 2: Reduced lOFC LFP oscillation power in *Sapap3* KO mice. (**A**) Averaged LFP power spectrogram of WT and *Sapap3* KO mice. Shading represents standard error of the mean. (**B**) Representative LFP raw recording traces from WT mice (black) and *Sapap3* KO mice (red). Traces were from mice with an LFP power spectrogram closest to the mean values of the corresponding groups. (**C**, **D**, **E**, **F**) Comparison of lOFC LFP oscillation power in δ, θ, β and γ bands between WT and *Sapap3* KO mice, respectively. *$p < 0.05$, ***$p < 0.001$, Wilcoxon rank sum test. Error bars represent standard error of the mean. KO = knockout; LFP = local field potential; lOFC = lateral orbitofrontal cortex; WT = wildtype.

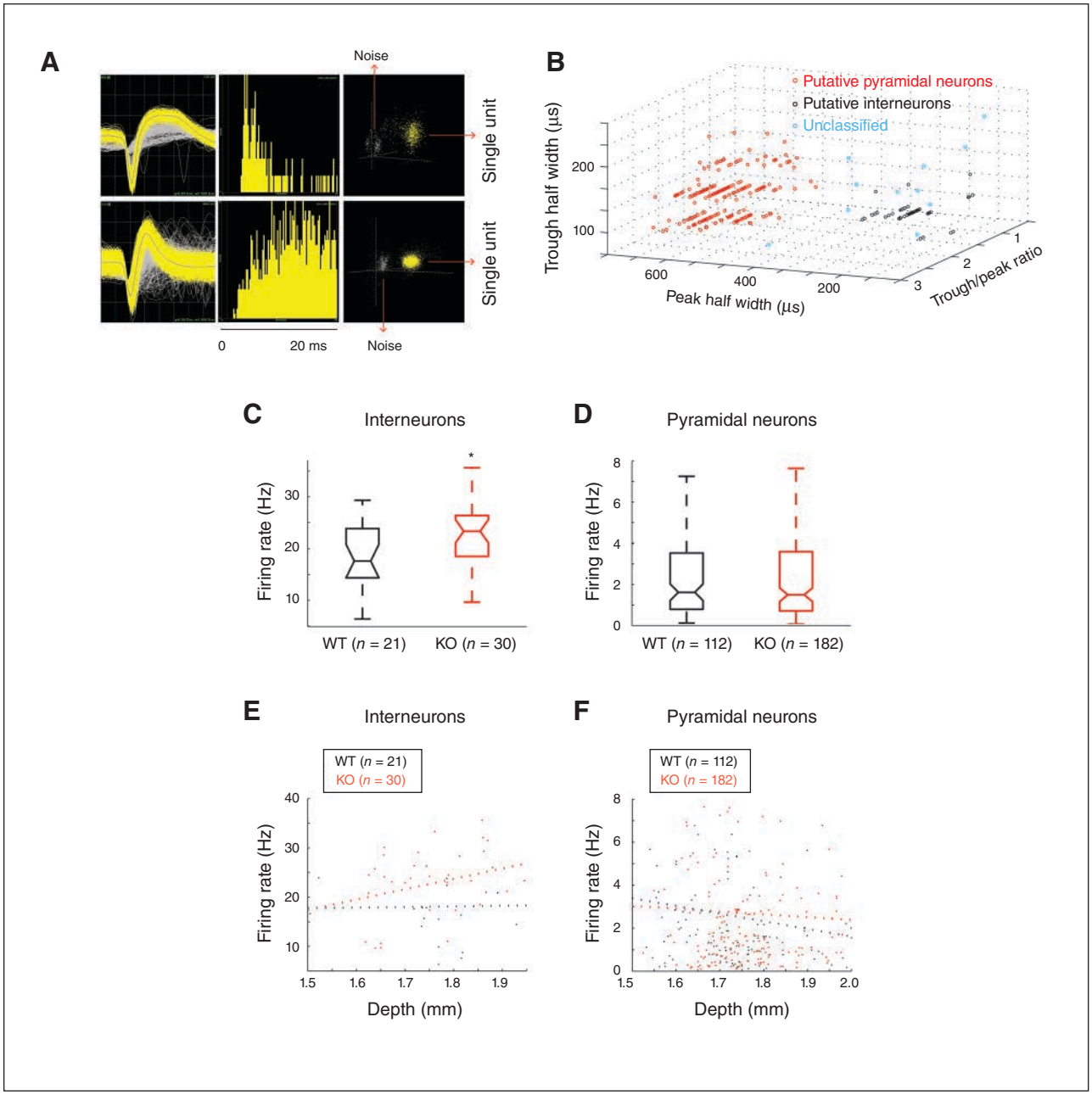

Fig. 3: The mean firing rate of lOFC putative interneurons increased in *Sapap3* KO mice, but the mean firing rate of putative pyramidal neurons did not change. (**A**, **B**) Isolation and classification of the recorded single units in lOFC. (**A**) Top panel: an example of an isolated putative pyramidal single unit in lOFC. Bottom panel: an example of an isolated putative interneuron single unit in lOFC. Left to right: overlay of the waveforms of the isolated single unit (yellow) and the noise waveforms (grey). Interspike interval histogram. Projection of the clusters correspondent to the unit and the noise (*x* axis: PC1, *y* axis: PC2, *z* axis: nonlinear energy). (**B**) Three-dimensional scatter plot illustrating spike characteristics of all 362 single units recorded in the lOFC of WT and *Sapap3* KO mice. Each unit is represented as a dot for peak width at half-peak amplitude (*x* axis), trough width at half trough amplitude (*y* axis) and ratio of trough to peak amplitude (*z* axis). We identified 2 major clusters. Putative pyramidal neurons are shown in red. Putative interneurons are shown in black. Units that did not meet the criteria for these classifications are shown in blue. (**C**) The mean firing rate of putative interneurons increased in *Sapap3* KO mice (red) compared to WT mice (black); **p* = 0.02, Wilcoxon rank sum test. (**D**) The mean firing rate of putative pyramidal neurons was similar between WT (black) and *Sapap3* KO (red) mice; *p* = 0.63, Wilcoxon rank sum test. The whiskers in the box plots cover 95% of the data. (**E**) We found no correlation between interneuron firing rate and depth. Spearman rank correlation coefficient: WT, *r* = 0.02, *p* = 0.94; KO, *r* = 0.29, *p* = 0.12. (**F**) We found no correlation between pyramidal neuron firing rate and depth. Spearman rank correlation coefficient: WT, *r* = –0.15, *p* = 0.11; KO, *r* = –0.04, *p* = 0.57. KO = knockout; lOFC = lateral orbitofrontal cortex; PC = principal component; WT = wildtype.

we adopted a method that was less sensitive to firing rate fluctuation over time than the coefficient of variation of ISIs.[41] This method compared only adjacent ISIs by calculating C_{V2} for adjacent ISIs (see Methods).

Neurons cannot fire as variably at a high rate as at a low rate because of the refractory period. To avoid comparing the periods when the neuron fires quickly with periods when the neuron fires slowly, we did not compute the mean C_{V2} over the entire recording period. Instead, we computed the mean C_{V2} for different ISI values. Both lOFC putative pyramidal neurons and interneurons in *Sapap3* KO mice exhibited enhanced discharge variability for ISIs from 10–190 ms compared to WT mice ($p_{FWE} < 0.001$ for both putative pyramidal neurons and putative interneurons, Wilcoxon rank sum test for each ISI range; family-wise error rate was calculated to correct for multiple comparisons; Fig. 5). Cortical neurons typically fire action potentials with high temporal precision.[44] Change of the spike timing influences information coding in several sensory modalities, such as olfaction,[45] gustation,[46] audition[47] and vision.[48] The increased discharge variability of pyramidal neurons and interneurons interferes with normal information coding and processing in OFC and may reflect circuitry abnormalities for OCD-like behaviours.

Altered synchronization of lOFC putative pyramidal neurons and interneurons in Sapap3 *KO mice*

Temporal precision of firing and a tightly maintained balance between excitation and inhibition is critical to normal neural synchronization. Because we observed altered firing variability

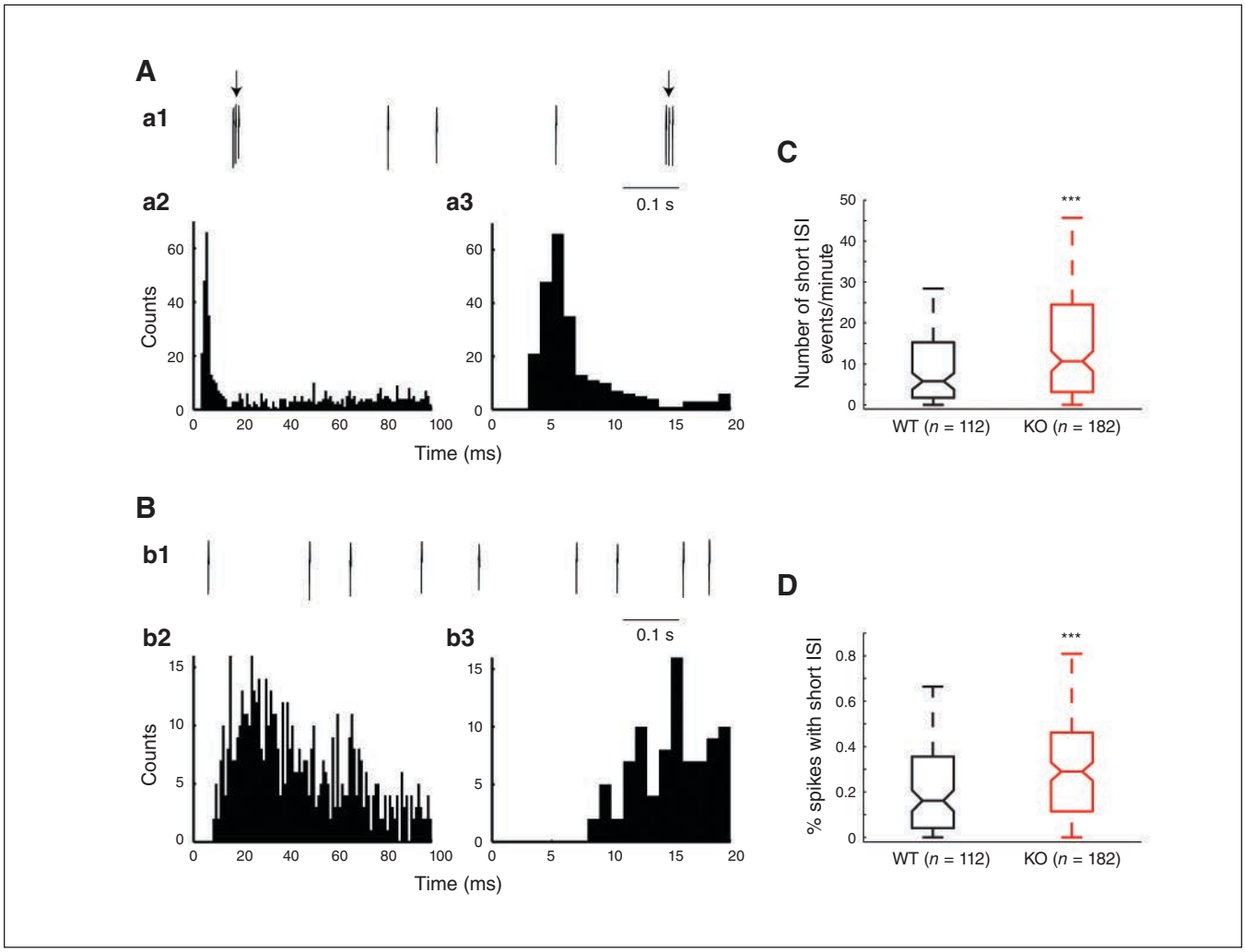

Fig. 4: The lOFC putative pyramidal neurons showed increased bursting activity in *Sapap3* KO mice. (**A**) A representative example of bursty pyramidal neurons in *Sapap3* KO mice: a1 shows the raw recording trace showing 2 bursts with short intra-burst ISI (intra-burst ISI < 10 ms, shown by arrows); a2 shows ISI distribution (bin size 1 ms); a3 shows an enlarged view of the ISI distribution from 0–20 ms to better demonstrate the short intra-burst ISI. (**B**) A representative example of non-bursty pyramidal neurons in *Sapap3* KO mice. (**C**) The number of bursts per minute per neuron increased in *Sapap3* KO mice; ***p = 0.001, Wilcoxon rank sum test. (**D**) The percentage of spikes per neuron in the bursting mode increased in *Sapap3* KO mice; ***p < 0.001; Wilcoxon rank sum test. The whiskers in the box plots cover 95% of the data. KO = knockout; ISI = interspike interval; lOFC = lateral orbitofrontal cortex; WT = wildtype.

and distinct perturbations of excitatory and inhibitory neurons, we then sought to investigate whether the levels of synchronous activity in lOFC would change in *Sapap3* KO mice by calculating the STA of LFP. Because the LFP averages over many neurons, STA is more sensitive than cross-correlation in detecting local neuronal synchronization.[49] Troughs in STA of LFP correspond to depolarization of intracellularly measured membrane potential, reflecting summed excitatory events in a pool of neurons. Upward deflections in STA of LFP correspond to a drop in membrane potential.[50] In both WT and *Sapap3* KO mice, lOFC putative pyramidal neurons and interneurons all fired preferentially at the lowest point of the trough. The percentage of cells entrained to the LFP oscillations as measured by significant fluctuations in the STA around the time of spike was similar between WT and *Sapap3* KO mice (WT putative pyramidal neurons 70.6 ± 9.5% mean ± SEM, KO putative pyramidal neurons 72.0 ± 7.0%, $p = 0.9$, Wilcoxon rank sum test; WT putative interneurons 96.4 ± 3.9%, KO putative interneurons 100%, $p = 0.9$, Wilcoxon rank sum test). However, the shape of averaged STA of both putative pyramidal neurons and interneurons differed in *Sapap3* KO mice. The central trough of the STA of both putative pyramidal neurons and interneurons was reduced in *Sapap3* KO mice (Fig. 6). This reduction may have been due to the reduced power of LFP oscillation in *Sapap3* KO mice. In WT mice, the averaged STA of putative interneurons exhibited a broad second peak after the central trough (Fig. 6A). This peak was significantly reduced in *Sapap3* KO mice, indicating that interneurons experienced less synchronized inhibition after firing a spike. The peak ahead of the central trough of the STA of putative pyramidal neurons was eliminated in *Sapap3* KO mice (Fig. 6B), indicating that synchronized inhibition on membrane potential, which sculpts the time window when an action potential can occur, was reduced in *Sapap3* KO mice. As a result, in *Sapap3* KO mice, the spike timing of individual lOFC pyramidal neurons may become less accurate. This was consistent with our finding that the firing variability of lOFC putative pyramidal neurons increased in *Sapap3* KO mice. Taken together, the changes in synchrony, along with the spike activity pattern and LFP changes reported in previous sections, point to the lOFC as a malfunctioning neural substrate for behavioural phenotypes relevant to OCD.

Discussion

Cognitive and executive function requires the coordinated activity of large-scale networks. Deficits in temporal coordination in the OFC can lead to disruption of its normal function and be involved in the pathophysiology of OCD. In the present study, we have reported alterations in LFP oscillations in the lOFC of an OCD mouse model, to our knowledge, for the first time. Specifically, we found that *Sapap3* KO mice exhibited reduced power in δ, θ, β and γ oscillations at rest. The neural substrates contributing to the different frequency bands of LFP oscillations and the mechanisms by which these oscillations are generated are not well understood. Therefore, a mechanistic interpretation of how the altered activity pattern of lOFC pyramidal neurons and interneurons contributes to decreased LFP oscillations in multiple frequency bands is challenging. Nevertheless, changes in neuronal activity synchronization do contribute to LFP oscillation alterations. We found that putative interneurons experienced less synchronized inhibition after firing an action potential and putative pyramidal neurons experienced less synchronized inhibition before firing an action potential. This reduced synchronous activity in the lOFC may contribute to decreased LFP oscillation power in multiple frequency bands. Consistent with our results, animal studies have shown that deep-brain stimulation of the nucleus accumbens, which can effectively alleviate OCD symptoms, elevated spontaneous LFP oscillation power in the δ, β and γ frequency bands in the OFC in rats.[51,52] In contrast, low-frequency deep-brain stimulation of the nucleus accumbens, which is ineffective in OCD, exerted no effect on LFP in the OFC.[51,52] Given that LFP oscillation power in the OFC was decreased in an OCD mouse model and increased with deep-brain stimulation of the nucleus accumbens in rats, alterations in LFP may serve as a potential neurophysiological biomarker to be further examined in people with OCD.

Inhibitory interneurons form reciprocal connections broadly with pyramidal neurons, and so are well positioned to coordinate the timing of pyramidal cell activity, regulate information processing and gate information flow. Compromised cortical inhibitory interneurons have been implicated in multiple psychiatric and neurologic disorders, including schizophrenia,[53] autism[54] and epilepsy.[55] However, little research on interneurons has been done in people with OCD or in animal models. It has been reported that *Sapap3* KO mice have a decreased number of PV-expressing interneurons in the centromedial striatum.[37] For the first time, our work found elevated spontaneous activity and enhanced discharge variability of putative inhibitory interneurons in the lOFC of *Sapap3* KO mice. Because the lOFC directly projects to the striatum, inhibition is disrupted in both parts of the cortical–striatal circuit in this OCD mouse model. Inhibitory interneurons are critical for the normal function of the OFC. The activity of inhibitory interneurons in the OFC showed strong behaviour correlates.[56] Compromised inhibitory interneurons in the OFC altered pyramidal neuron activity correlations with decision and reward, and impaired reversal learning.[40] The activity alterations of interneurons we found may disrupt the normal function of the lOFC and help identify one aspect of malfunction in this region for behaviours relevant to OCD. Interneurons also play a fundamental role in rhythmogenesis. The elevated spontaneous activity and discharge variability of interneurons may be causally involved in the LFP alterations in lOFC, as we found in *Sapap3* KO mice. Alternatively, the increased spontaneous activity of interneurons could represent adaptive, homeostatic or unrelated processes to compensate for other primary abnormalities of the lOFC in *Sapap3* KO mice.

Although the OFC is thought to play a critical role in OCD, there are discrepancies in the directionality of findings about how the baseline activity of the OFC is altered in people with OCD or animal models. These discrepancies may be due to several factors, including the heterogeneity of the disorder,

comorbidities, medication history and the different subdivisions of OFC analyzed. Our study excluded these confounders by focusing on the lOFC in an OCD mutant mouse model, and with clear classification of different cell types. Two studies have assessed OFC activity change in OCD mouse models. One found that the baseline activity of lOFC putative pyramidal neurons measured by electrophysiological recording was similar between WT and *Sapap3* KO mice,[37] consistent with our results. The other reported upregulated baseline activity in the OFC in *Slitrk5* KO mice measured by FosB expression.[57] Because this study relied on molecular markers of cell activity, we do not know the details of activity pattern change for

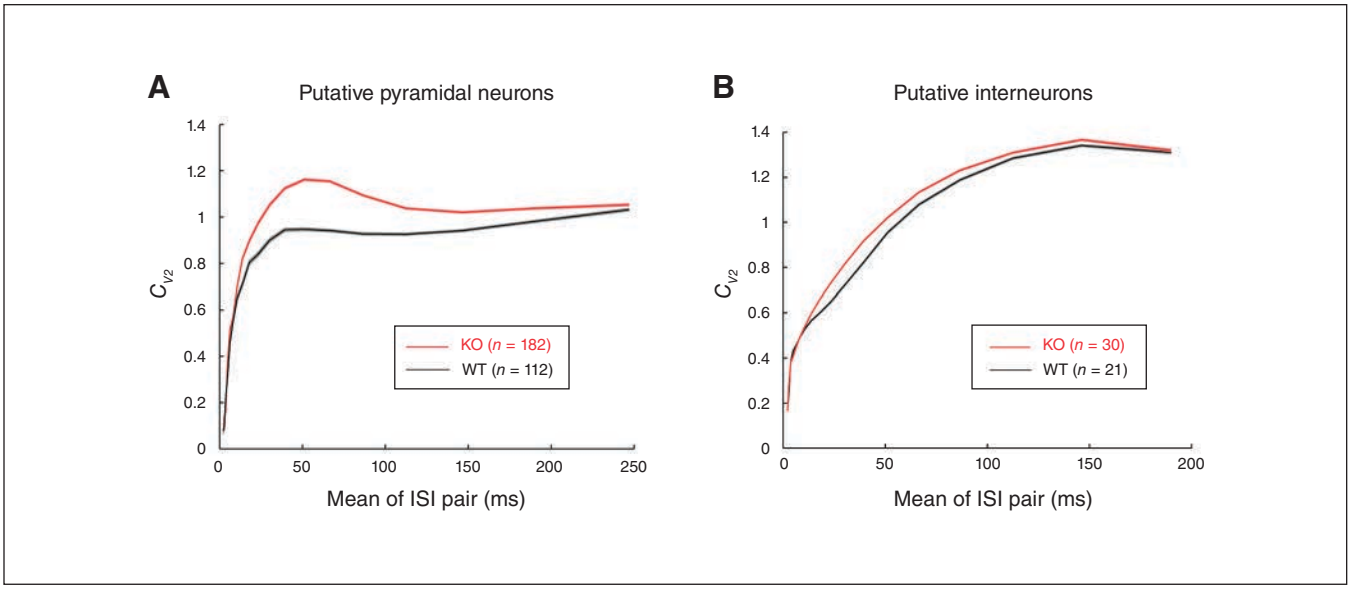

Fig. 5: The lOFC putative pyramidal neurons and interneurons exhibited enhanced discharge variability in *Sapap3* KO mice (red) compared to WT littermates (black). (**A**) Mean C_{V2} of lOFC putative pyramidal neurons plotted against the mean of the 2 adjacent ISIs used to compute C_{V2}. (**B**) Mean C_{V2} of lOFC putative interneurons plotted against the mean of the 2 adjacent ISIs used to compute C_{V2}. The *x* axis is the mean of the 2 adjacent ISIs used to compute C_{V2}. The lines are the mean C_{V2} values in logarithmically spaced bins. The ratio between bin boundaries was 1.3. We chose logarithmic binning because the upper limit of C_{V2} at shorter ISIs changes much more rapidly than at longer ISIs. Shading represents standard error of the mean. KO = knockout; ISI = interspike interval; lOFC = lateral orbitofrontal cortex; WT = wildtype.

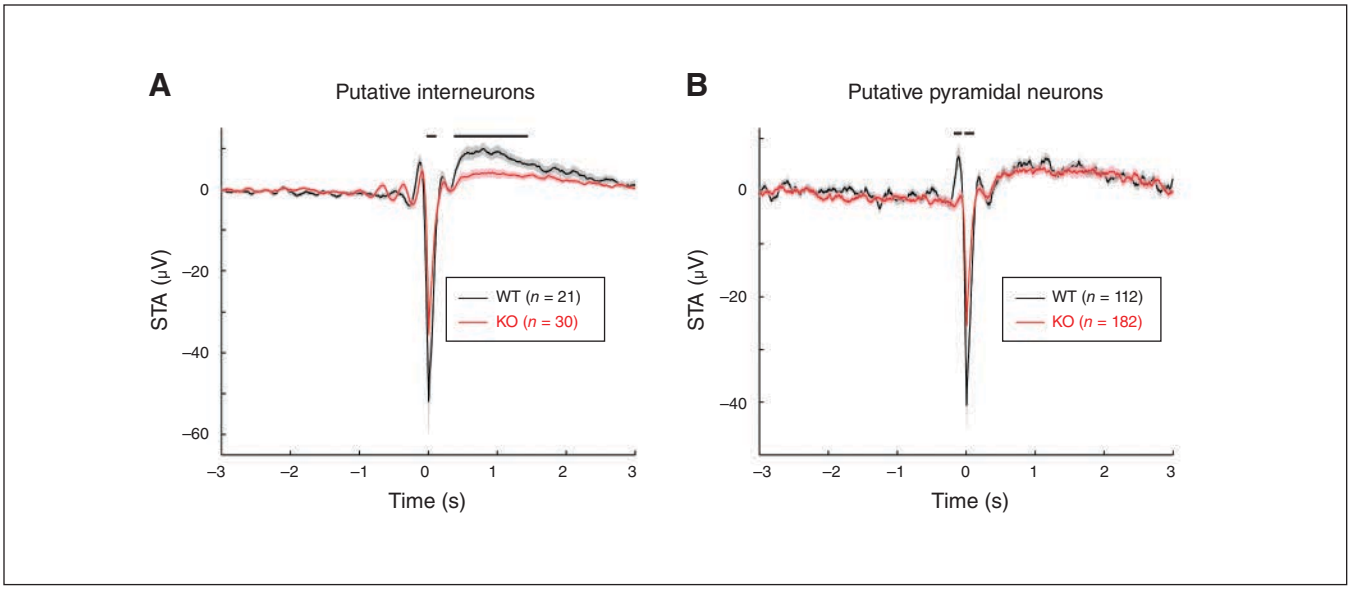

Fig. 6: Comparisons of lOFC ensemble synchronization in WT (black) and *Sapap3* KO (red) mice. (**A**) Averaged STA of LFP of lOFC putative interneurons. (**B**) Average STA of LFP of lOFC putative pyramidal neurons. Black horizontal bars indicate ranges with significant difference between WT and *Sapap3* KO mice. Shading represents standard error of the mean. KO = knockout; LFP = local field potential; lOFC = lateral orbitofrontal cortex; STA = spike-triggered average; WT = wildtype.

specific neuronal types. The increased bursting activity of putative pyramidal neurons we found could cause this increase in FosB expression. The discrepancy may also result from the different OCD animal models used (*Sapap3* KO v. *Slitrk5* KO), different cell types (putative pyramidal neurons v. all cells) and different subregions of the OFC examined (lOFC v. the entire OFC). The medial and lateral OFC perform different functions, such as processing positive versus negative valence.[35,36] The activity of these 2 subregions may be differentially affected in OCD mouse models, giving rise to inconsistent results when examining the lOFC versus the entire OFC.

Although the mean firing rate of lOFC pyramidal neurons was similar between WT and *Sapap3* KO mice, their activity pattern changed dramatically in *Sapap3* KO mice. Specifically, lOFC pyramidal neurons exhibited significantly increased bursting activity with short intra-burst ISI (< 10 ms). Overall activity pattern determines neuronal function, not merely firing rate. Bursts with short intra-burst ISI have special importance in brain function. Compared with tonic firing, burst firing is more reliable for eliciting synaptic transmission, provides stronger output, enhances signal-to-noise ratio and facilitates synaptic plasticity.[43] The increased bursting activity of lOFC pyramidal neurons may provide pathologic stronger output through the OFC–striatal circuit and drive increased activity in the striatum of *Sapap3* KO mice, as reported in previous studies.[37,58] Another study suggested that sustained increase in synaptic strength from the OFC pyramidal neurons to ventral striatum synapses led to increased repetitive behaviour in mice.[59] Many clinical and animal studies have suggested that hyperactivity in the cortico–striato–thalamo–cortical circuit is associated with OCD pathology.[2,3,10,11] The enhanced bursting activity of lOFC pyramidal neurons may drive hyperactivity in the cortico–striato–thalamo–cortical circuit and contribute to OCD-like behaviours in *Sapap3* KO mice. A recent study reported that a depression-like state depended critically on a bursting mode of firing in the lateral habenula in rats and mice.[60] The bursting activity of neurons in the lateral habenula was greatly enhanced in rat and mouse models of depression, and reducing their bursting activity elicited antidepressant effects. Increasing bursting activity by optogenetics was sufficient to induce depression-like behaviours. This study suggested that abnormal bursting activity in a single nucleus could lead to symptoms relevant to a psychiatric disorder. Abnormal bursting activity has not been studied in people with OCD or in animal models. In a future study, we plan to investigate whether fluoxetine can suppress the abnormal bursting activity of lOFC pyramidal neurons, accompanied by alleviation of OCD-like behaviours in *Sapap3* KO mice. We also plan to investigate whether artificially increasing the bursting activity of lOFC pyramidal neurons can induce symptoms relevant to OCD.

Limitations

One limitation of this study was that we examined activity pattern alterations of lOFC neurons only when the mice were resting; we did not examine grooming-related activity. As an association cortex, the OFC performs complex cognitive and executive brain functions. Its neuronal activity is modulated by many behaviours, including grooming-associated movements themselves. To exclude such confounders, we compared neuronal activity between WT and *Sapap3* KO mice, recorded only when the mice were stationary. To collect enough data during stationary periods, we applied a head-fixed configuration instead of a free-behaviour configuration, because mice stayed stationary for most of the time during head-fixed recording (percent of time spent stationary, mean ± SEM: WT 90.1 ± 2.3%, KO 90.8 ± 3.5%). In contrast, mice usually moved most of the time during free-movement recording (including both locomotion and fine movement), leaving few stationary periods for effective data analysis. Comparing resting neuronal activity between WT and *Sapap3* KO mice required very high recording and spike-sorting quality. We applied very strict criteria for spike sorting and included only very well isolated single units to ensure the accuracy of our results. Specifically, the cluster of the isolated single unit had to be well separated from other clusters without any overlapping of the edge, because edge overlapping in spike sorting results in contamination by other units or loss of spikes of the isolated unit. Either situation can significantly affect the measurement of firing rate and firing variability. Another limitation was that we investigated functional abnormalities without establishing causality for these functional changes and the OCD-like behaviours. Our reasons were as follows. First, this was a pioneering in vivo electrophysiological study of OFC dysfunction in an OCD animal model; characterizing the functional abnormalities was the first step and can serve an important foundation for future work. Second, artificially generating bursts with very short intra-burst ISI without changing the mean firing rate is very challenging; we have not found an appropriate way to manipulate the oscillation power of broad frequency bands in the LFP without changing the mean firing rate of excitatory neurons. Nevertheless, causal manipulation is definitely a key future experiment that may require us to develop new manipulation techniques.

Conclusion

Here, we have provided the first direct in vivo electrophysiological evidence of detailed functional alterations in different neuronal types and local network dysfunction in the lOFC in phenotypes relevant to OCD. These findings advance our understanding of the neuropathophysiology and circuitry mechanisms that underlie OCD-like behaviours, and may help generate and refine hypotheses for further investigation. For example, the LFP alterations and increased bursting activity may be useful biomarker candidates for further examination in people with OCD.

Acknowledgements: We thank Dr. Kathleen B. Quast for her comments on the manuscript. This work was supported by grants from the National Natural Science Foundation of China (grant no. 31371108, 31171051), the Natural Science Foundation of Beijing (grant no. 5132007, 5112008), the General Program of Science and Technology Development Project of Beijing Municipal Education Commission of China (grant no. KM201110025001), the Beijing

Municipal Technology Foundation for Selected Overseas Chinese Scholars, the Simons Initiative on Autism and the Brain Infrastructure Grant Program.

Affiliations: From the Department of Neurobiology, Beijing Institute for Brain Disorders, Beijing Centre of Neural Regeneration and Repair, Key Laboratory for Neurodegenerative Diseases of the Ministry of Education, Capital Medical University, Beijing, China (Lei, Lai, Sun, Xu); the McGovern Institute for Brain Research, Department of Brain and Cognitive Sciences, Massachusetts Institute of Technology, Cambridge, Massachusetts (Feng); and the Stanley Center for Psychiatric Research, Broad Institute of MIT and Harvard, Cambridge, Massachusetts (Feng).

Competing interests: None declared.

Contributors: H. Lei, Q. Xu and G. Feng designed the study. H. Lei, J. Lai and X. Sun acquired the data, which H. Lei and J. Lai analyzed. H. Lei and G. Feng wrote the article, which all authors reviewed. All authors approved the final version to be published and can certify that no other individuals not listed as authors have made substantial contributions to the paper.

References

1. Ruscio AM, Stein DJ, Chiu WT, et al. The epidemiology of obsessive–compulsive disorder in the National Comorbidity Survey Replication. *Mol Psychiatry* 2010;15:53-63.
2. Monteiro P, Feng G. Learning from animal models of obsessive–compulsive disorder. *Biol Psychiatry* 2016;79:7-16.
3. Burguiere E, Monteiro P, Mallet L, et al. Striatal circuits, habits, and implications for obsessive–compulsive disorder. *Curr Opin Neurobiol* 2015;30:59-65.
4. Ahmari SE. Using mice to model obsessive compulsive disorder: from genes to circuits. *Neuroscience* 2016;321:121-37.
5. Pittenger C, Bloch MH, Williams K. Glutamate abnormalities in obsessive compulsive disorder: neurobiology, pathophysiology, and treatment. *Pharmacol Ther* 2011;132:314-32.
6. Boedhoe PS, Schmaal L, Abe Y, et al. Distinct subcortical volume alterations in pediatric and adult OCD: a worldwide meta- and mega-analysis. *Am J Psychiatry* 2016;174:60-9.
7. Anticevic A, Hu S, Zhang S, et al. Global resting-state functional magnetic resonance imaging analysis identifies frontal cortex, striatal, and cerebellar dysconnectivity in obsessive–compulsive disorder. *Biol Psychiatry* 2014;75:595-605.
8. Breiter HC, Rauch SL. Functional MRI and the study of OCD: from symptom provocation to cognitive-behavioral probes of cortico-striatal systems and the amygdala. *Neuroimage* 1996;4:S127-38.
9. Milad MR, Rauch SL. Obsessive–compulsive disorder: beyond segregated cortico-striatal pathways. *Trends Cogn Sci* 2012;16:43-51.
10. Del Casale A, Kotzalidis GD, Rapinesi C, et al. Functional neuroimaging in obsessive–compulsive disorder. *Neuropsychobiology* 2011;64:61-85.
11. Menzies L, Chamberlain SR, Laird AR, et al. Integrating evidence from neuroimaging and neuropsychological studies of obsessive–compulsive disorder: the orbitofronto-striatal model revisited. *Neurosci Biobehav Rev* 2008;32:525-49.
12. Menzies L, Achard S, Chamberlain SR, et al. Neurocognitive endophenotypes of obsessive–compulsive disorder. *Brain* 2007;130:3223-36.
13. Baxter MG, Parker A, Lindner CC, et al. Control of response selection by reinforcer value requires interaction of amygdala and orbital prefrontal cortex. *J Neurosci* 2000;20:4311-9.
14. Schoenbaum G, Nugent SL, Saddoris MP, et al. Orbitofrontal lesions in rats impair reversal but not acquisition of go, no-go odor discriminations. *Neuroreport* 2002;13:885-90.
15. Schoenbaum G, Roesch MR, Stalnaker TA, et al. A new perspective on the role of the orbitofrontal cortex in adaptive behaviour. *Nat Rev Neurosci* 2009;10:885-92.
16. Gillan CM, Papmeyer M, Morein-Zamir S, et al. Disruption in the balance between goal-directed behavior and habit learning in obsessive–compulsive disorder. *Am J Psychiatry* 2011;168:718-26.
17. Chamberlain SR, Menzies L, Hampshire A, et al. Orbitofrontal dysfunction in patients with obsessive–compulsive disorder and their unaffected relatives. *Science* 2008;321:421-2.
18. Alptekin K, Degirmenci B, Kivircik B, et al. Tc-99m HMPAO brain perfusion SPECT in drug-free obsessive–compulsive patients without depression. *Psychiatry Res* 2001;107:51-6.
19. Baxter LR Jr, Schwartz JM, Mazziotta JC, et al. Cerebral glucose metabolic rates in nondepressed patients with obsessive–compulsive disorder. *Am J Psychiatry* 1988;145:1560-3.
20. Rubin RT, Villanueva-Meyer J, Ananth J, et al. Regional xenon 133 cerebral blood flow and cerebral technetium 99m HMPAO uptake in unmedicated patients with obsessive–compulsive disorder and matched normal control subjects. Determination by high-resolution single-photon emission computed tomography. *Arch Gen Psychiatry* 1992;49:695-702.
21. Sawle GV, Hymas NF, Lees AJ, et al. Obsessional slowness. Functional studies with positron emission tomography. *Brain* 1991; 114:2191-202.
22. Swedo SE, Schapiro MB, Grady CL, et al. Cerebral glucose metabolism in childhood-onset obsessive–compulsive disorder. *Arch Gen Psychiatry* 1989;46:518-23.
23. Cottraux J, Gerard D, Cinotti L, et al. A controlled positron emission tomography study of obsessive and neutral auditory stimulation in obsessive–compulsive disorder with checking rituals. *Psychiatry Res* 1996;60:101-12.
24. Rauch SL, Jenike MA, Alpert NM, et al. Regional cerebral blood flow measured during symptom provocation in obsessive–compulsive disorder using oxygen 15-labeled carbon dioxide and positron emission tomography. *Arch Gen Psychiatry* 1994;51:62-70.
25. Andreou C, Leicht G, Popescu V, et al. P300 in obsessive–compulsive disorder: source localization and the effects of treatment. *J Psychiatr Res* 2013;47:1975-83.
26. Benkelfat C, Nordahl TE, Semple WE, et al. Local cerebral glucose metabolic rates in obsessive–compulsive disorder. Patients treated with clomipramine. *Arch Gen Psychiatry* 1990;47:840-8.
27. Le Jeune F, Verin M, N'Diaye K, et al. Decrease of prefrontal metabolism after subthalamic stimulation in obsessive–compulsive disorder: a positron emission tomography study. *Biol Psychiatry* 2010;68:1016-22.
28. Nakao T, Nakagawa A, Yoshiura T, et al. Brain activation of patients with obsessive–compulsive disorder during neuropsychological and symptom provocation tasks before and after symptom improvement: a functional magnetic resonance imaging study. *Biol Psychiatry* 2005;57:901-10.
29. Saxena S, Brody AL, Maidment KM, et al. Localized orbitofrontal and subcortical metabolic changes and predictors of response to paroxetine treatment in obsessive–compulsive disorder. *Neuropsychopharmacology* 1999;21:683-93.
30. Swedo SE, Pietrini P, Leonard HL, et al. Cerebral glucose metabolism in childhood-onset obsessive–compulsive disorder. Revisualization during pharmacotherapy. *Arch Gen Psychiatry* 1992; 49:690-4.
31. Welch JM, Lu J, Rodriguiz RM, et al. Cortico-striatal synaptic defects and OCD-like behaviours in *Sapap3*-mutant mice. *Nature* 2007;448:894-900.
32. Boardman L, van der Merwe L, Lochner C, et al. Investigating SAPAP3 variants in the etiology of obsessive–compulsive disorder and trichotillomania in the South African white population. *Compr Psychiatry* 2011;52:181-7.
33. Zuchner S, Wendland JR, Ashley-Koch AE, et al. Multiple rare SAPAP3 missense variants in trichotillomania and OCD. *Mol Psychiatry* 2009;14:6-9.
34. Stewart SE, Yu D, Scharf JM, et al. Genome-wide association study of obsessive–compulsive disorder. *Mol Psychiatry* 2013;18:788-98.
35. Milad MR, Rauch SL. The role of the orbitofrontal cortex in anxiety disorders. *Ann N Y Acad Sci* 2007;1121:546-61.
36. Kringelbach ML, Rolls ET. The functional neuroanatomy of the human orbitofrontal cortex: evidence from neuroimaging and neuropsychology. *Prog Neurobiol* 2004;72:341-72.
37. Burguiere E, Monteiro P, Feng G, et al. Optogenetic stimulation of lateral orbitofronto-striatal pathway suppresses compulsive behaviors. *Science* 2013;340:1243-6.
38. Dombeck DA, Khabbaz AN, Collman F, et al. Imaging large-scale neural activity with cellular resolution in awake, mobile mice. *Neuron* 2007;56:43-57.
39. Zhan C, Luo M. Diverse patterns of odor representation by neurons in the anterior piriform cortex of awake mice. *J Neurosci* 2010;30: 16662-72.

40. Bissonette GB, Schoenbaum G, Roesch MR, et al. Interneurons are necessary for coordinated activity during reversal learning in orbitofrontal cortex. *Biol Psychiatry* 2015;77:454-64.
41. Holt GR, Softky WR, Koch C, et al. Comparison of discharge variability in vitro and in vivo in cat visual cortex neurons. *J Neurophysiol* 1996;75:1806-14.
42. Pogarell O, Juckel G, Mavrogiorgou P et al. Symptom-specific EEG power correlations in patients with obsessive-compulsive disorder. *Int J Psychophysiol* 2006;62:87-92.
43. Lisman JE. Bursts as a unit of neural information: making unreliable synapses reliable. *Trends Neurosci* 1997;20:38-43.
44. Mainen ZF, Sejnowski TJ. Reliability of spike timing in neocortical neurons. *Science* 1995;268:1503-6.
45. Wehr M, Laurent G. Odour encoding by temporal sequences of firing in oscillating neural assemblies. *Nature* 1996;384:162-6.
46. Roussin AT, D'Agostino AE, Fooden AM, et al. Taste coding in the nucleus of the solitary tract of the awake, freely licking rat. *J Neurosci* 2012;32:10494-506.
47. Lu T, Liang L, Wang X. Temporal and rate representations of time-varying signals in the auditory cortex of awake primates. *Nat Neurosci* 2001;4:1131-8.
48. Rathbun DL, Alitto HJ, Weyand TG, et al. Interspike interval analysis of retinal ganglion cell receptive fields. *J Neurophysiol* 2007;98:911-9.
49. Fries P, Reynolds JH, Rorie AE, et al. Modulation of oscillatory neuronal synchronization by selective visual attention. *Science* 2001; 291:1560-3.
50. Steriade M. Grouping of brain rhythms in corticothalamic systems. *Neuroscience* 2006;137:1087-106.
51. McCracken CB, Grace AA. High-frequency deep brain stimulation of the nucleus accumbens region suppresses neuronal activity and selectively modulates afferent drive in rat orbitofrontal cortex in vivo. *J Neurosci* 2007;27:12601-10.
52. McCracken CB, Grace AA. Nucleus accumbens deep brain stimulation produces region-specific alterations in local field potential oscillations and evoked responses in vivo. *J Neurosci* 2009; 29:5354-63.
53. Lewis DA, Hashimoto T, Volk DW. Cortical inhibitory neurons and schizophrenia. *Nat Rev Neurosci* 2005;6:312-24.
54. Lawrence YA, Kemper TL, Bauman ML, et al. Parvalbumin-, calbindin-, and calretinin-immunoreactive hippocampal interneuron density in autism. *Acta Neurol Scand* 2010;121:99-108.
55. Aronica E, Redeker S, Boer K, et al. Inhibitory networks in epilepsy-associated gangliogliomas and in the perilesional epileptic cortex. *Epilepsy Res* 2007;74:33-44.
56. Quirk MC, Sosulski DL, Feierstein CE, et al. A defined network of fast-spiking interneurons in orbitofrontal cortex: responses to behavioral contingencies and ketamine administration. *Front Syst Neurosci* 2009;3:13.
57. Shmelkov SV, Hormigo A, Jing D, et al. *Slitrk5* deficiency impairs corticostriatal circuitry and leads to obsessive–compulsive-like behaviors in mice. *Nat Med* 2010:16:598-602.
58. Mintzopoulos D, Gillis TE, Robertson HR, et al. Striatal magnetic resonance spectroscopy abnormalities in young adult SAPAP3 knockout mice. *Biol Psychiatry Cogn Neurosci Neuroimaging* 2016;1:39-48.
59. Ahmari SE, Spellman T, Douglass NL, et al. Repeated cortico-striatal stimulation generates persistent OCD-like behavior. *Science* 2013;340:1234-9.
60. Yang Y, Cui YH, Sang KN, et al. Ketamine blocks bursting in the lateral habenula to rapidly relieve depression. *Nature* 2018; 554:317.